

Light field distribution of general function photonic crystals

Xiang-Yao Wu^a, Bo-Jun Zhang^a, Xiao-Jing Liu^a

Si-Qi Zhang^a, Jing Wang^a, Nuo Ba^a, Li Xiao^a and Hong Li^a

^a*Institute of Physics, Jilin Normal University, Siping 136000, China*

In this paper, We have presented a new general function photonic crystals (GFPCs), which refractive indexes are line functions of space position in two mediums A and B , and obtain new results: (1) when the line function of refractive indexes is up or down, the transmissivity can be far larger or smaller than 1. (2) when the refractive indexes function increase or decrease along the direction of incident light, the light intensity should be magnified or weaken, which can be made optical magnifier or attenuator. (3) The GFPCs can be made optical diode when the light positive and negative incident the GFPCs.

PACS: 42.70.Qs, 78.20.Ci, 41.20.Jb

Keywords: General Photonic crystals; Transmissivity; Optical diode; Optical magnifier

PACS numbers:

1. Introduction

Photonic crystals (PC) are a new kind of materials which facilitate the control of the light [1-5]. An important feature of the photonic crystals is that there are allowed and forbidden ranges of frequencies at which light propagates in the direction of index periodicity [6-9]. Due to the forbidden frequency range, known as photonic band gap (PBG) [10-15], which forbids the radiation propagation in a specific range of frequencies. The existence of PBGs will lead to many interesting phenomena. In the past ten years has been developed an intensive effort to study and micro-fabricate PBG materials in one, two or three dimensions, e.g., modification of spontaneous emission [16-19] and photon localization [20-23]. Reduction or suppression of the density of states within the band gap facilitates light localization and trapping in a bulk material [24-25], as well as the inhibition of spontaneous emission over a broad frequency range. Thus numerous applications of photonic crystals have been proposed in improving the performance of optoelectronic and microwave devices such as high-efficiency semiconductor lasers, light emitting diodes, wave guides, optical filters, high-Q resonators, antennas, frequency-selective surface, optical limiters and amplifiers [26-27].

In Ref. [28], we have proposed special function photonic crystals, which the medium refractive index is the function of space position, but the function value of refractive index is equal at two endpoints of every medium A and B . In Ref. [29], we have proposed a new general function photonic crystals, i.e., the medium refractive index is a arbitrary function of space position, and find the transmissivity of one-dimensional GFPCs can be much larger or smaller than 1 for different slope linearity refractive index function. In this paper, we choose two linearity refractive index functions for two medium A and B , and give the light field distribution in the GFPCs. We obtain some new results: (1) when the line function of refractive indexes is up, the transmissivity can be far larger than 1. (2) when the line function of refractive indexes is down, the transmissivity can be far smaller than 1. (3) when the two-endpoint values of refractive index are equal for mediums A and B , the transmissivity T is in the range of 0 and 1 (it becomes conventional PCs). So, the conventional PCs is the special case of the GFPCs. (4) when the refractive indexes function increase along the direction of incident light, the light intensity should be magnified, which can be made light magnifier. (5) when the refractive indexes function decrease along the direction of incident light, the light intensity should be weaken, which can be made light attenuator. (5) The GFPCs can be made light diode. The general function photonic crystals can be applied to design more optical instruments.

(3) when the two-endpoint values of refractive index are equal for mediums A and B , the transmissivity T is in the range of 0 and 1 (it becomes conventional PCs). So, the conventional PCs is the special case of the GFPCs. (4) when the refractive indexes function increase along the direction of incident light, the light intensity should be magnified, which can be made light magnifier. (5) when the refractive indexes function decrease along the direction of incident light, the light intensity should be weaken, which can be made light attenuator. (5) The GFPCs can be made light diode. The general function photonic crystals can be applied to design more optical instruments.

2. The light motion equation in general function photonic crystals

For the general function photonic crystals, the medium refractive index is a periodic function of the space position, which can be written as $n(z)$, $n(x, z)$ and $n(x, y, z)$ corresponding to one-dimensional, two-dimensional and three-dimensional function photonic crystals. In the following, we shall deduce the light motion equations of the one-dimensional general function photonic crystals, i.e., the refractive index function is $n = n(z)$, meanwhile motion path is on xz plane. The incident light wave strikes plane interface point A , the curves AB and BC are the path of incident and reflected light respectively, and they are shown in FIG. 1.

The light motion equation can be obtained by Fermat principle, it is

$$\delta \int_A^B n(z) ds = 0. \quad (1)$$

In the two-dimensional transmission space, the line element ds is

$$ds = \sqrt{(dx)^2 + (dz)^2} = \sqrt{1 + \dot{z}^2} dx, \quad (2)$$

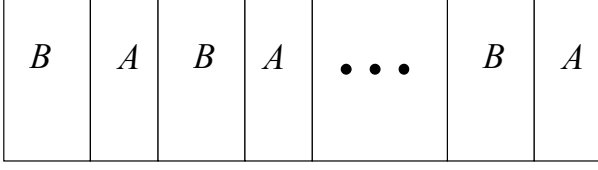


FIG. 3: The structure $(BA)^N$ of the general function photonic crystals.

where $k_0 = \cot \theta_t^I$ and $k_z = \frac{dz}{dx}$. From Eq. (12), there is $n(z) > n(0) \sin \theta_t^I$, and the coordinate x_B is

$$x_B = x_A + \int_0^b \frac{dz}{\sqrt{(1 + k_0^2)(\frac{n(z)}{n(0)})^2 - 1}}, \quad (14)$$

where b is the medium thickness of FIG. 1 and FIG. 2. By substituting Eqs. (9) and (14) into (10), and using the equality

$$n(0) \sin \theta_t^I = n(b) \sin \theta_i^I, \quad (15)$$

we have

$$E_{i2} = E_{t1} e^{i\delta_b}, \quad (16)$$

where

$$\delta_b = \frac{\omega}{c} n_b(b) (\cos \theta_i^I b + \sin \theta_i^I \int_0^b \frac{dz}{\sqrt{\frac{n_b^2(z)}{n_0^2 \sin^2 \theta_i^I} - 1}}), \quad (17)$$

and similarly

$$E'_{r2} = E_{r2} e^{i\delta_b}. \quad (18)$$

Substituting Eqs. (16) and (18) into (7) and (8), and using $H = \sqrt{\frac{\varepsilon_0}{\mu_0}} n E$, we obtain

$$\begin{pmatrix} E_I \\ H_I \end{pmatrix} = M_B \begin{pmatrix} E_{II} \\ H_{II} \end{pmatrix}, \quad (19)$$

where

$$M_B = \begin{pmatrix} \cos \delta_b & -\frac{i \sin \delta_b}{\sqrt{\frac{\varepsilon_0}{\mu_0}} n_b(b) \cos \theta_i^I} \\ -i n_b(0) \sqrt{\frac{\varepsilon_0}{\mu_0}} \cos \theta_i^I \sin \delta_b & \frac{n_b(0) \cos \theta_i^I \cos \delta_b}{n_b(b) \cos \theta_i^I} \end{pmatrix} \quad (20)$$

The Eq. (20) is the transfer matrix M in the medium of FIG. 1 and FIG. 2. By refraction law, we can obtain

$$\sin \theta_t^I = \frac{n_0}{n(0)} \sin \theta_i^0, \cos \theta_t^I = \sqrt{1 - \frac{n_0^2}{n^2(0)} \sin^2 \theta_i^0}, \quad (21)$$

where n_0 is air refractive index, and $n(0) = n(z)|_{z=0}$. Using Eqs. (15) and (21), we can calculate $\cos \theta_i^I$.

4. The transmissivity and light field distribution of one-dimensional general function photonic crystals

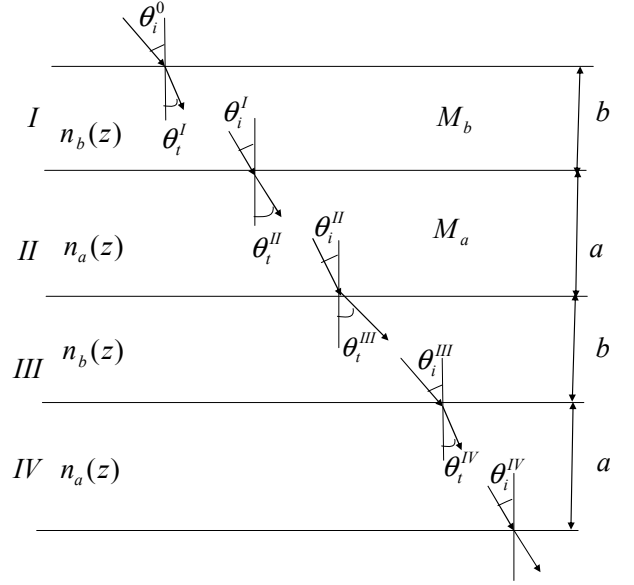


FIG. 4: The two periods transmission figure of light in general function photonic crystals.

In section 3, we obtain the M matrix of the half period. We know that the conventional photonic crystals are constituted by two different refractive index medium, and the refractive indexes are not continuous on the interface of the two mediums. We could devise the one-dimensional general function photonic crystals structure as follows: in the first half period, the refractive index distributing function of medium B is $n_b(z)$, and in the second half period, the refractive index distributing function of medium A is $n_a(z)$, corresponding thicknesses are b and a , respectively. Their refractive indexes satisfy condition $n_b(b) \neq n_a(0)$, their structures are shown in FIG. 3, and FIG. 4. The Eq. (20) is the half period transfer matrix of medium B . Obviously, the half period transfer matrix of medium A is

$$M_A = \begin{pmatrix} \cos \delta_a & -\frac{i \sin \delta_a}{\sqrt{\frac{\varepsilon_0}{\mu_0}} n_a(a) \cos \theta_i^{II}} \\ -i n_a(0) \sqrt{\frac{\varepsilon_0}{\mu_0}} \cos \theta_i^{II} \sin \delta_a & \frac{n_a(0) \cos \theta_i^{II} \cos \delta_a}{n_a(a) \cos \theta_i^{II}} \end{pmatrix} \quad (22)$$

where

$$\delta_a = \frac{\omega}{c} n_a(a) [\cos \theta_i^{II} \cdot a + \sin \theta_i^{II} \int_0^a \frac{dz}{\sqrt{\frac{n_a^2(z)}{n_0^2 \sin^2 \theta_i^0} - 1}}], \quad (23)$$

$$\cos \theta_t^{II} = \sqrt{1 - \frac{n_0^2}{n_a^2(0)} \sin^2 \theta_i^0}, \quad (24)$$

and

$$\sin \theta_i^{II} = \frac{n_0}{n_a(a)} \sin \theta_i^0, \quad (25)$$

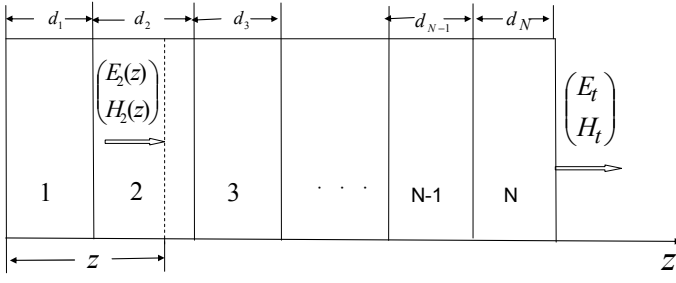


FIG. 5: The input and output light in the GFPCs.

$$\cos \theta_i^{II} = \sqrt{1 - \frac{n_0^2}{n_a^2(a)} \sin^2 \theta_i^0}. \quad (26)$$

In one period, the transfer matrix M is

$$M = M_B \cdot M_A = \begin{pmatrix} \cos \delta_b & \frac{-i \sin \delta_b}{\sqrt{\frac{\epsilon_0}{\mu_0}} n_b(b) \cos \theta_i^I} \\ -i n_b(0) \sqrt{\frac{\epsilon_0}{\mu_0}} \cos \theta_t^I \sin \delta_b & \frac{n_b(0) \cos \theta_t^I \cos \delta_b}{n_b(b) \cos \theta_i^I} \end{pmatrix} \begin{pmatrix} \cos \delta_a & \frac{-i \sin \delta_a}{\sqrt{\frac{\epsilon_0}{\mu_0}} n_a(a) \cos \theta_i^{II}} \\ -i n_a(0) \sqrt{\frac{\epsilon_0}{\mu_0}} \cos \theta_t^{II} \sin \delta_a & \frac{n_a(0) \cos \theta_t^{II} \cos \delta_a}{n_a(a) \cos \theta_i^{II}} \end{pmatrix} \quad (27)$$

The form of the GFPCs transfer matrix M is more complex than the conventional PCs. The angle θ_i^I , θ_t^I , θ_i^{II} and θ_t^{II} are shown in Fig. 4. The characteristic equation of GFPCs is

$$\begin{aligned} \begin{pmatrix} E_1 \\ H_1 \end{pmatrix} &= M_1 M_2 \cdots M_N \begin{pmatrix} E_{tN+1} \\ H_{tN+1} \end{pmatrix} \\ &= M_b M_a M_b M_a \cdots M_b M_a \begin{pmatrix} E_{tN+1} \\ H_{tN+1} \end{pmatrix} \\ &= M \begin{pmatrix} E_{tN+1} \\ H_{tN+1} \end{pmatrix} = \begin{pmatrix} A & B \\ C & D \end{pmatrix} \begin{pmatrix} E_{tN+1} \\ H_{tN+1} \end{pmatrix} \end{aligned} \quad (28)$$

Where N is the period number. With the transfer matrix M (Eq. (28)), we can obtain the transmission and reflection coefficient t and r , and the transmissivity and reflectivity T and R , they are

$$t = \frac{E_{tN+1}}{E_{0i}} = \frac{2\eta_0}{A\eta_0 + B\eta_0\eta_{N+1} + C + D\eta_{N+1}}, \quad (29)$$

$$r = \frac{E_{0r}}{E_{0i}} = \frac{A\eta_0 + B\eta_0\eta_{N+1} - C - D\eta_0}{A\eta_0 + B\eta_0\eta_{N+1} + C + D\eta_0}, \quad (30)$$

and

$$T = t \cdot t^*, \quad (31)$$

$$R = r \cdot r^*. \quad (32)$$

Where $\eta_0 = \eta_{N+1} = \sqrt{\frac{\epsilon_0}{\mu_0}}$, E_{0i} and E_{0r} are incident and reflection electric field, and $E_1 = E_{0i} + E_{0r}$. In the

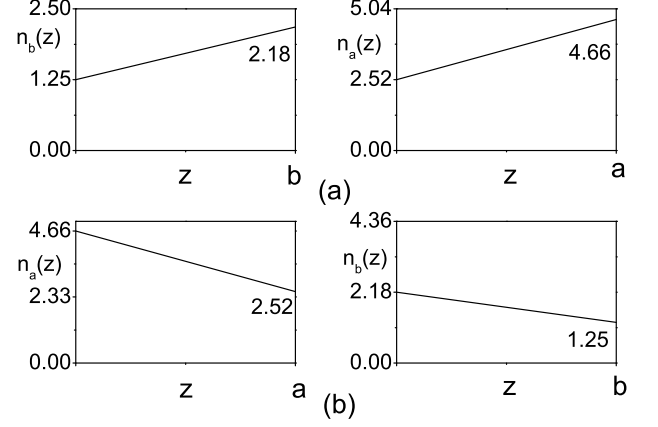


FIG. 6: The line refractive index functions in a period. The FIG. 6(a) is the up line function of refractive indexes, and FIG. 6(b) is the down line function of refractive indexes.

following, we give the electric field distribution of light in the one-dimensional GFPCs, and the propagation figure of light is shown in FIG. 5. From Eq. (28), we have

$$\begin{aligned} \begin{pmatrix} E_2(z) \\ H_2(z) \end{pmatrix} &= M_1(d_1) M_2(d_2 - z) \cdots M_N(d_N) \begin{pmatrix} E_{tN+1} \\ H_{tN+1} \end{pmatrix} \\ &= \begin{pmatrix} A(z) & B(z) \\ C(z) & D(z) \end{pmatrix} \begin{pmatrix} E_{tN+1} \\ H_{tN+1} \end{pmatrix}. \end{aligned} \quad (33)$$

where d_1 and d_2 are the thickness of first and second medium, respectively, $E_2(z)$ and $H_2(z)$ are the electric field and magnetic field in the second medium, when position z changes we can obtain the electric field and magnetic field in other medium. The E_t and H_t are the transmission electric and magnetic field. Eq. (33) can be written as

$$\begin{aligned} E(z) &= A(z)E_{tN+1} + B(z)H_{tN+1} \\ &= A(z)E_{tN+1} + B(z)\sqrt{\frac{\epsilon_0}{\mu_0}}E_{tN+1} \\ &= (A(z) + B(z)\sqrt{\frac{\epsilon_0}{\mu_0}})tE_{0i}, \end{aligned} \quad (34)$$

and then

$$|\frac{E(z)}{E_{0i}}|^2 = |t|^2 |A(z) + B(z)\sqrt{\frac{\epsilon_0}{\mu_0}}|^2 \quad (35)$$

5. Numerical result

In this section, we report our numerical results of transmissivity. We consider refractive indexes of the linearity functions in a period, it is

$$n_b(z) = n_b(0) + \frac{n_b(b) - n_b(0)}{b}z, \quad 0 \leq z \leq b, \quad (36)$$

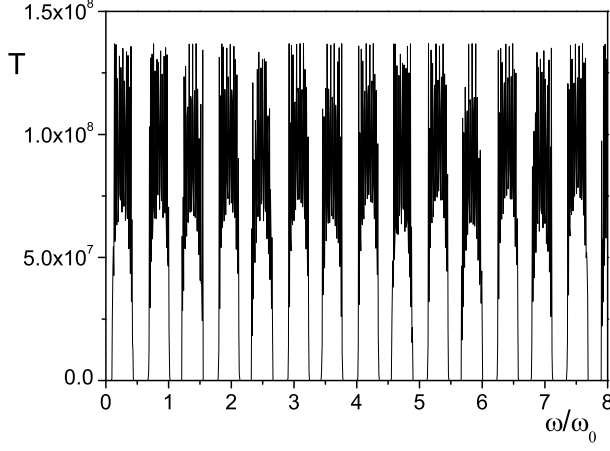


FIG. 7: The relation between transmissivity and frequency corresponding to the up line function of refractive indexes (FIG .6(a)).

$$n_a(z) = n_a(0) + \frac{n_a(a) - n_a(0)}{a}z, \quad 0 \leq z \leq a, \quad (37)$$

Eqs. (36) and (37) are the line refractive indexes distribution functions of two half period mediums B and A . When the endpoint values $n_b(0)$, $n_b(b)$, $n_a(0)$ and $n_a(a)$ are all given, the line refractive index functions $n_b(z)$ and $n_a(z)$ are ascertained. The main parameters are: the half period thickness b and a , the starting point refractive indexes $n_b(0)$ and $n_a(0)$, and end point refractive indexes $n_b(b)$ and $n_a(a)$, the optical thickness of the two mediums are equal, i.e., $n_b(0)b = n_a(0)a$, the incident angle $\theta_i^0 = 0$, the center frequency $\omega_0 = 1.215 \times 10^{15} Hz$, the thickness $b = 310nm$, $a = 154nm$ and the period number $N = 16$, i.e., the structure of GFPCs is $(BA)^{16}$.

In FIG. 5(a), we take $n_b(0) = 1.25$, $n_b(b) = 2.18$ for the medium B , and $n_a(0) = 2.52$, $n_a(a) = 4.66$ for the medium A , which are the up line function of refractive indexes. In FIG. 5(b), we take $n_b(0) = 2.18$, $n_b(b) = 1.25$ for the medium B , and $n_a(0) = 4.66$, $n_a(a) = 2.52$ for the medium A , which are the down line function of refractive indexes. By the refractive indexes function, we can calculate the transmissivity. With the FIG. 6(a) and 6(b), we obtain the transmissivity distribution in FIG. (7) and FIG. (8) respectively. From FIG. (7) and FIG. (8), we obtain the results: (1) when the line function of refractive indexes is up, the transmissivity can be far larger than 1 (T maximum is 10^8). (2) when the line function of refractive indexes is down, the transmissivity can be far smaller than 1 (T maximum is 10^{-9}), which are different from the transmissivity of conventional PCs ($0 \leq T \leq 1$). These results are inexplicable and doubtful even, but they are correct. When we take $n_b(0) = n_b(b) = 1.25$ and $n_a(0) = n_a(a) = 2.52$, i.e., two-endpoint values of refractive index are equal for mediums A and B (it is conventional PCs), and by the Eq. (27), (30) and (32),

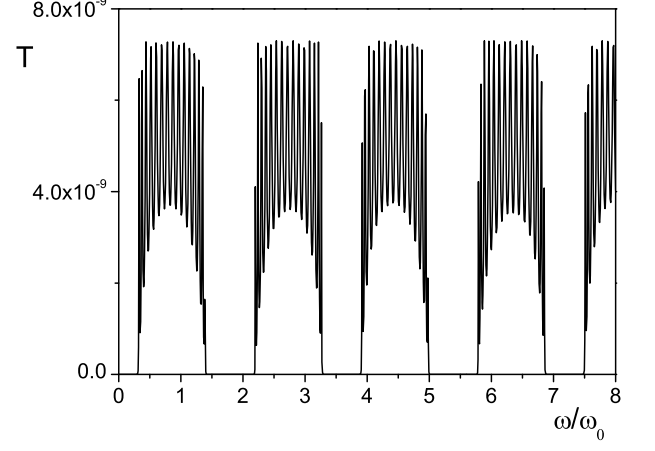


FIG. 8: The relation between transmissivity and frequency corresponding to the down line function of refractive indexes (FIG .6(b)).

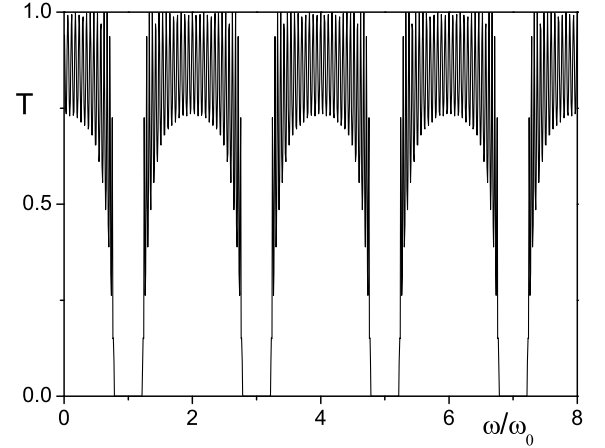


FIG. 9: The relation between transmissivity and frequency for the GFPCs, when the two-endpoint values of refractive index are equal

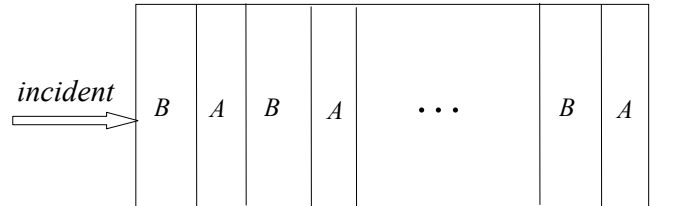


FIG. 10: The light positive incident to the GFPCs.

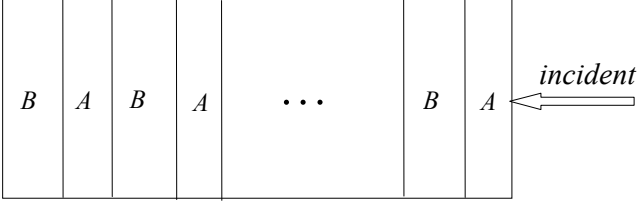


FIG. 11: The light negative incident to the GFPCs.

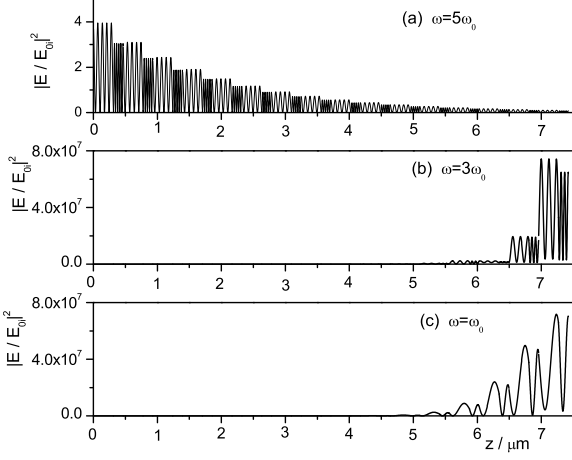


FIG. 12: The light distribution of positive incident (FIG. 10) in the GFPCs. Figure (a) (b) and (c) are corresponding to the incident light frequency $\omega = \omega_0$, $3\omega_0$ and $5\omega_0$.

we obtain the transmissivity distribution in FIG. (9), its transmissivity T is in the range of 0 and 1 (it becomes conventional PCs transmissivity distribution). So, the conventional PCs is the special case of the GFPCs.

In the following, we shall study the light field distribution of the one-dimensional GFPCs for the positive and negative incident of light. The positive incident figure is shown in FIG. 10, and the negative incident is shown in FIG. 11, which relative to the positive incident FIG. 10. The refractive indexes line function of positive incident is in FIG. 6(a), and the FIG. 6(b) is the refractive indexes line function of negative incident corresponding to the positive incident FIG. 6(a). From Eq. (35), we can calculate the electric field distribution in the GFPCs. Figures 12 and 13 are the electric field distributions of positive incident (FIG. 10). In FIG. 12, the frequency of incident light ω is the odd times of the center frequency ω_0 . In FIG. 12 (a), (b) and (c), the incident light ω are corresponding to ω_0 , $3\omega_0$ and $5\omega_0$. When $\omega = \omega_0$ and $3\omega_0$, the light intensity of transmission are enhanced or magnified (magnification $M = 10^7$), while $\omega = 5\omega_0$, the intensity of transmission light is weaken. From FIG. 7, we can find when $\omega = \omega_0$ and $3\omega_0$ the light is in conductance band, and the transmission light has been enhanced by the GFPCs. In the conventional PCs, the intensity of

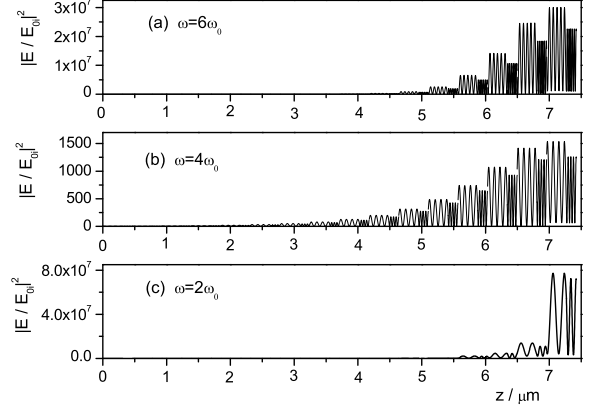


FIG. 13: The light distribution of positive incident (FIG. 10) in the GFPCs. Figure (a) (b) and (c) are corresponding to the incident light frequency $\omega = 2\omega_0$, $4\omega_0$ and $6\omega_0$.

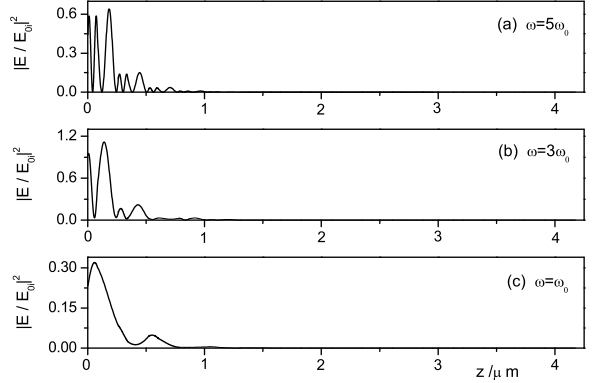


FIG. 14: The light distribution of negative incident (FIG. 11) in the GFPCs. Figure (a) (b) and (c) are corresponding to the incident light frequency $\omega = \omega_0$, $3\omega_0$ and $5\omega_0$.

transmission light can not be magnified. When $\omega = 5\omega_0$ the light is in forbidden band, and the transmission light has been weaken by the GFPCs. In FIG. 13, the frequency of incident light ω is the even times of the center frequency ω_0 . In FIG. 13 (a), (b) and (c), the incident light ω are corresponding to $2\omega_0$, $4\omega_0$ and $6\omega_0$, the intensities of transmission light have been magnified. Figures 14 and 15 are the electric field distributions of negative incident (FIG. 11). In Figures. 14 and 15, the frequency of incident light ω is the odd and even times of the center frequency ω_0 , and the intensities of transmission light have been all weaken. By calculation, we can obtain the following results for the GFPCs: (1) For the positive incident, i.e., the refractive indexes increasing along the direction of incident light, the intensity of transmission light have been magnified when the incident light frequency is in conductance band, which can be made light

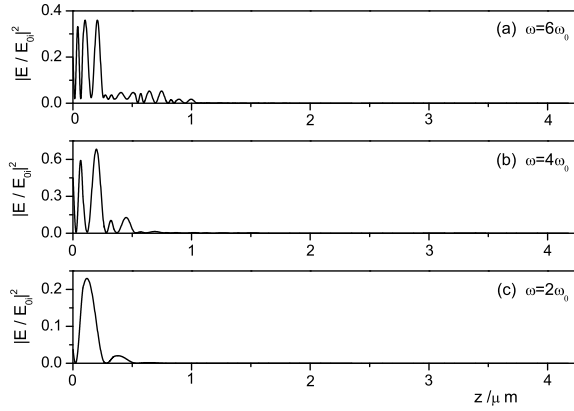


FIG. 15: The light distribution of negative incident (FIG. 11) in the GFPCs. Figure (a) (b) and (c) are corresponding to the incident light frequency $\omega = 2\omega_0$, $4\omega_0$ and $6\omega_0$.

magnifier (magnifying multiple 10^7). (2) For the negative incident, i.e., the refractive indexes decreasing along the direction of incident light, the intensity of transmission light have been weaken, which can be made light attenuator (magnifying multiple less than 1). (3) The GFPCs structure (positive incident FIG. 10 and negative incident FIG. 11) is the optical diode, since the light intensity is magnified (the light get across) when the light is positive

incident, and the light intensity has been decreased (the light cutoff) when the light is negative incident, which transmits light from an input to an output, but not in reverse direction.

6. Conclusion

In summary, We have theoretically investigated a new general function photonic crystals (GFPCs), which refractive index is an arbitrary function of space position. We choose the line refractive index function for two mediums A and B . By the calculation, We obtain the following results: (1) when the line function of refractive indexes is up, the transmissivity can be far larger than 1. (2) when the line function of refractive indexes is down, the transmissivity can be far smaller than 1. (3) when the two-endpoint values of refractive index are equal for mediums A and B , the transmissivity T is in the range of 0 and 1 (it becomes conventional PCs). So, the conventional PCs is the special case of the GFPCs. (4) when the refractive indexes function increase along the direction of incident light, the light intensity should be magnified, which can be made light magnifier. (5) when the refractive indexes function decrease along the direction of incident light, the light intensity should be weaken, which can be made light attenuator. (5) The GFPCs can be made light diode. The general function photonic crystals can be applied to design more optical instruments.

-
- [1] E. Yablonovitch, Phys. Rev. Lett. **58**, 2059-2062 (1987).
 - [2] P. Russell, Science **299**, 358-362 (2003).
 - [3] J. C. Knight, Nature **424**, 847-851 (2003).
 - [4] A. F. Abouraddy, M. Bayindir, G. Benoit, S. D. Hart, K. Kuriki, N. Orf, O. Shapira, F. Sorin, B. Temelkuranl, and Y. Fink, Nature Photonics **6**, 336-347 (2007).
 - [5] J. D. Joannopoulos, P. R. Villeneuve, and S. Fan, Nature **386**, 143-149 (1997).
 - [6] M. R. Jorgensen, J. W. Galusha, and M. H. Bart, Phys. Rev. Lett. **107**, 143902 (2011).
 - [7] S. John, Phys. Rev. Lett. **58**, 2486-2489 (1987).
 - [8] P. Nedel, X. Letartre, C. Seassal, A. Auffves, L. Ferrier, E. Drouard, A. Rahmani, and P. Viktorovitch., Optics Express. **19** 5014 (2011).
 - [9] M. D. Leistikow, A. P. Mosk, E. Yeganegi, S. R. Huisman, A. Lagendijk, and W. L. Vos, Phys. Rev. Lett. **107**, 193903 (2011).
 - [10] C. Zinoni, B. Alloing, L. H. Li, F. Marsili, A. Fiore, L. Lunghi, A. Gerardino, Yu. B. Vakhtomin, K. V. Smirnov, and G. N. Gol'tsman., Appl. Phys. Lett. **91** 031106 (2007).
 - [11] T. Yoshie, A. Scherer, J. Hendrickson, G. Khitrova, H. M. Gibbs, G. Rupper, C. Ell, O. B. Shchekin, and D. G. Deppe, Nature **432**, 200C203 (2004).
 - [12] K. Nozaki, S. Kita, and T. Baba, Opt. Express **15**, 7506C7514 (2007).
 - [13] S. G. Johnson and J. D. Joannopoulos., Optics Express. **8** 173 (2001).
 - [14] V. S. C. Manga Rao and S. Hughes., Phys. Rev. Lett. **99** 193901 (2007).
 - [15] G. Lecamp, P. Lalanne, and J. P. Hugonin., Phys. Rev. Lett. **99** 023902 (2007).
 - [16] V. S. C. Manga Rao and S. Hughes., Phys. Rev B **75** 205437 (2007).
 - [17] A. F. Koenderink and W. L. Vos, J. Opt. Soc. Am. B **22**, 1075C1084 (2005).
 - [18] M. L. M. Balistreri, H. Gersen, J. P. Korterik, L. Kuipers, and N. F. van Hulst, Science **294**, 1080C1082 (2001).
 - [19] S. I. Bozhevolnyi, V. S. Volkov, J. Arentoft, A. Boltas-seva, T. Sondergaard, and M. Kristensen, Opt. Commun. **212**, 51-55 (2002).
 - [20] T. Lund-Hansen, S. Stobbe, B. Julsgaard, H. Thyrrestrup, T. Snner, M. Kamp, A. Forchel, and P. Lodahl., Phys. Rev. Lett. **101** 113903 (2008).
 - [21] S. J. Dewhurst, D. Granados, D. J. P. Ellis, A. J. Bennett, R. B. Patel, I. Farrer, D. Anderson, G. A. C. Jones, D. A. Ritchie, and A. J. Shields., Appl. Phys. Lett. **96** 031109 (2010).
 - [22] K. Busch and S. John, Phys. Rev. Lett. **83**, 967 (1999).
 - [23] L. Okamoto, M. Loncar, T. Yoshie, A. Scherer, Y. Qiu, and P. Gogna, Appl. Phys. Lett. **82**, 1676-1678 (2003).
 - [24] P. Kramper, M. Agio, C. M. Soukoulis, A. Birner, F.

- Muller, R. B. Wehrspohn, U. Gosele, and V. Sandoghdar, Phys. Rev. Lett. **92**, 113903 (2004).
- [25] J-K. Yang, H. Noh, M. J. Rooks, G. S. Solomon, F. Vollmer and H. Cao., Appl. Phys. Lett. **98**, 241107 (2011).
- [26] R. Martinez-Sala, J. Sancho, J. V. Sanchez, V. Gomez, J. Llinares and F. Meseguer, nature **378**, 241 (1995).
- [27] D. Torrent, A. Hakansson, F. Cervera and J. Sanchez - Dehesa, Phys. Rev. Lett. **96**, 204302 (2006).
- [28] Xiang-Yao Wu, Bo-Jun Zhang, Jing-Hai Yang, Xiao-Jing Liu, Nuo Ba, Yi-Heng Wu and Qing-Cai Wang, Physica E **43**, 1694 (2011).
- [29] Xiang-Yao Wu, Bo-Jun Zhang, Jing-Hai Yang, Si-Qi Zhang, Xiao-Jing Liu, Jing Wang, Nuo Ba, Zhong Hua and Xin-Guo Yin, Accepted by Physica E.